

Entrainment Dynamics of Shear-Free Convective Boundary Layers Growing in Linearly and Discretely Stratified Fluids

R. Conzemius & E. Fedorovich

School of Meteorology, University of Oklahoma, Norman, Oklahoma, USA

INTRODUCTION

Boundary layers driven by surface buoyant forcings are commonly observed in the environmental flows. An atmospheric example of such boundary layer is the so-called convective boundary layer (CBL), which is driven by buoyancy production at the heated underlying surface during the daytime conditions. The buoyancy is defined as $b = -g(\rho - \rho_0)/\rho_0$, where ρ is the density of the fluid, ρ_0 is the reference density, and g is the acceleration due to gravity. In atmospheric terms, the buoyancy can be approximately expressed as $b = g(\theta_v - \theta_{v0})/\theta_{v0}$, where θ_v is the virtual potential temperature.

The CBL develops in the stably stratified environment of the earth atmosphere. In many instances, the buoyancy production of turbulence in the atmospheric CBL considerably dominates its production due to flow (wind) shears, so the CBL can be considered shear-free. The buoyant convective forcing generates up- and downward motions that effectively mix buoyancy (virtual potential temperature) field inside the CBL. In meteorology, the convective upward motions (updrafts) are commonly referred to as thermals. The fast rising warm thermals occupy less percentage of the CBL horizontal cross-sectional area than broader, but slower and cooler, descending convective downdrafts. Due to mixing associated with convective up- and downdrafts, the buoyancy field in the main portion of the CBL (the so-called convectively mixed layer) does not change considerably with height when averaged over horizontal planes or over time. Relatively large vertical gradients in the averaged buoyancy profile are observed close to the CBL top, throughout the interfacial (sub)layer that separates CBL from the stably stratified atmosphere aloft. A more buoyant air from the free atmosphere is entrained across this interfacial layer (also called the capping inversion layer, or simply – the capping inversion) into the convectively mixed flow region as the CBL grows. Such convective entrainment is maintained by flow disturbances resulting from the penetration of convective thermals into the stably stratified fluid above the CBL.

The CBL growth rate and the entrainment dynamics essentially depend on the stratification of quiescent fluid (free atmosphere), in which the CBL grows. This stratification can be continuous as well as discrete in the vertical. The particular case of continuous linear stratification corresponds to a constant buoyancy (virtual potential temperature) gradient in the fluid above

the density interface. The discrete stratification is characteristic of a multilayer fluid with discontinuities of the buoyancy gradient at the interfaces between layers.

During the last decade, the numerical large eddy simulation (LES) technique has been extensively applied to study convective entrainment in the continuously and linearly stratified atmosphere with and without wind shears, see review in by Stevens and Lenschow [1]. However, even for the case of shear-free CBL, a consensus has not been reached so far regarding the dependence of the integral parameters of entrainment on the capping inversion strength and stability in the quiescent fluid above the CBL. These integral parameters are the CBL growth rate (also called the entrainment rate), the entrainment ratio (the ratio of the heat flux of entrainment to the surface heat flux), and the relative entrainment layer depth (the ratio of the of entrainment layer depth to that of the CBL). Previous numerical studies of convective entrainment have often been handicapped by resolution and domain size limitations, which to date have prevented investigations of parameter variations over sufficiently wide ranges of free-atmosphere stratification and CBL depth.

The convective entrainment in the discretely stratified fluid has been studied much less. There is evidence, however, coming from experimental studies of the CBL [2] that in this case the nonstationarity of entrainment process plays an important role, and the CBL evolution passes through a sequence of transition stages accompanied by strong variations of the entrainment parameters [3].

In the present study, regimes of convective entrainment in linearly and discretely stratified fluids have been investigated by means of a high-resolution LES in conjunction with relevant data from atmospheric, laboratory, and other numerical studies.

EMPLOYED LES TECHNIQUE

The LES code used by Fedorovich *et al.* [4] to simulate the case of horizontally evolving CBL has been converted for the present study into the periodic-domain mode. The Boussinesq approximation is employed in the code to account for the buoyancy forcing on the resolved scales of motion. The subgrid turbulent fluxes are expressed in terms of the subgrid eddy viscosity/diffusivity concept. The viscosity and diffusivity coefficients are taken proportional to the product of the square root of subgrid turbulence kinetic energy (STKE) and the length scale of subgrid turbulence. The STKE is calculated from a separate balance equation that directly takes into account the contribution of subgrid buoyancy flux to the energy production. The length scale is taken equal to the effective grid cell size in the convective flow region and parameterized through the STKE and the buoyancy frequency in the stably stratified portion of the flow. The Monin-Obukhov similarity relationships are used to relate parameters of momentum and heat transport at the heated underlying surface.

The LES experiments have been conducted in a rectangular domain with the vertical-to-horizontal dimension ratio equal to 4/5, on two grids containing alternatively 100×100×200 and 50×50×200 rectangular cells (the latter numbers correspond to the vertical direction), with

constant horizontal and vertical spacing. In order to minimize the effect of the upper boundary, the linear sponge layer has been introduced in the upper one fifth of the simulation domain and the maximum allowed ratio of the CBL depth to the domain height has been set equal to 0.6. This provides 12/25 as the upper limit for the ratio of the CBL depth to the domain width.

ENTRAINMENT IN LINEARLY STRATIFIED FLUID

We first consider the average profiles of buoyancy b and vertical kinematic turbulent buoyancy flux B in the shear-free CBL that develops in a linearly stratified fluid heated from below, see Fig. 1. Three regions (sublayers) can be distinguished within the CBL: the near-surface layer, whose depth is typically very small compared to the overall CBL depth, the convectively mixed layer, and the inversion layer. Very close to the surface, the buoyancy decreases with height from its surface value to its value in the mixed layer, where the buoyancy field is approximately height-constant. The buoyancy flux B decreases linearly with height in the mixed layer, and its zero-crossing height as will be shown below corresponds to the mixed layer top. Above the mixed layer, b increases sharply with height throughout the capping inversion layer, whilst B reaches a minimum at level z_i within this layer and vanishes towards its upper boundary. The fluid above the CBL is linearly stratified with the vertical buoyancy gradient $db/dz=N^2$, where z is the height and N is the Brunt-Väisälä (buoyancy) frequency.

Convective entrainment in the linearly stratified atmosphere has been extensively studied using the zero-order jump model (ZOM) described, *e.g.*, in Lilly [5] and Zilitinkevich [6]. In the ZOM of CBL, the interfacial (inversion) layer is replaced by a zero-order discontinuity interface with a buoyancy jump Δb at the inversion level z_i , which is taken as the CBL top. The negative entrainment buoyancy flux in the zero-order model is presented by $B_i = -\Delta b \cdot (dz_i/dt)$, where t is time. The most comprehensive ZOM of the shear-free CBL was developed by Zilitinkevich [6], who has shown that z_i and Δb are universal functions of dimensionless time $\hat{t} = tN$ when scaled with N and B_s : $\hat{z}_i = z_i B_s^{-1/2} N^{3/2} = \hat{z}_i(\hat{t})$ and $\hat{\Delta b} = \Delta b B_s^{-1/2} N^{-1/2} = \hat{\Delta b}(\hat{t})$. For the regime of equilibrium entrainment, when $\hat{z}_i(\hat{t})$ and $\hat{\Delta b}(\hat{t})$ do not depend on initial conditions and the energy flux from the CBL top can be neglected, Zilitinkevich [6] obtained: $\hat{z}_i = [2(1+2C_\epsilon)\hat{t}]^{1/2}$, $\hat{\Delta b} = C_\epsilon [2\hat{t}/(1+2C_\epsilon)]^{1/2}$, where $C_\epsilon \approx 0.2$ is a universal constant (the so-called entrainment coefficient) estimated in [6] from atmospheric and laboratory data. It is easy to see that in the considered entrainment regime the ZOM gives: $(\hat{\Delta b} \cdot \hat{z}_i)/(2\hat{t}) = \hat{\Delta b}(d\hat{z}_i/d\hat{t}) = \Delta b(dz_i/dt)/B_s = -B_i/B_s = C_\epsilon$.

The following dimensionless combinations are commonly used in meteorology and fluid dynamics to parameterize the convective entrainment in a linearly stratified fluid. The *dimensionless entrainment rate* $E = (dz_i/dt)/w_*$, where $w_* = (z_i B_s)^{1/3}$ is the Deardorff [7] convective velocity scale, the *Richardson number* $Ri_N = (z_i^2 N^2)/w_*^2$ based on the N value in the

turbulence-free fluid, and the *Richardson number* $Ri_b = (\Delta b \cdot z_i) / w_*^2$ based on the ZOM buoyancy increment Δb .

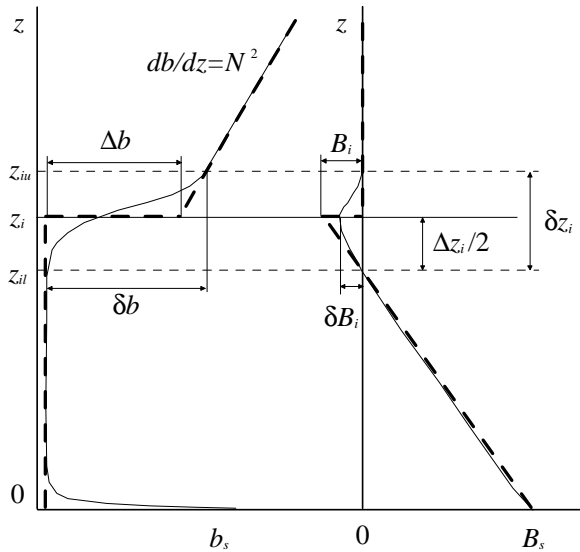


Figure 1. Representation of the buoyancy b and buoyancy flux B profiles in the zero-order jump model (ZOM), after Fedorovich and Mironov [3]). The actual b and B profiles are shown by thin solid lines and their ZOM counterparts are given by heavy dashed lines. See text for the notation.

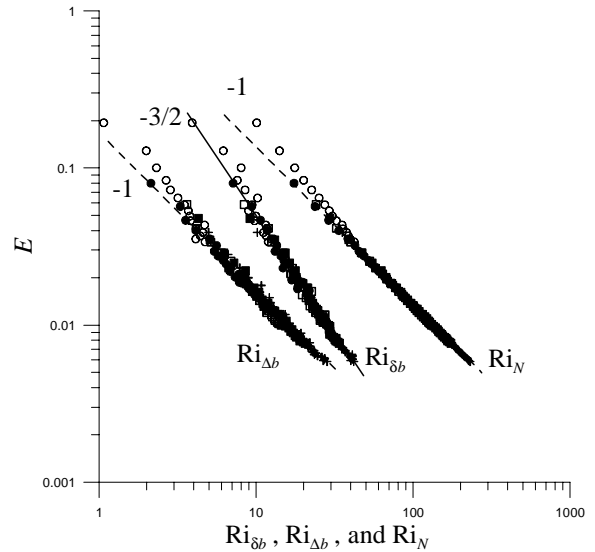


Figure 2. Relationships between entrainment parameters in a linearly stratified fluid. Symbols are the LES data for different N (open circles: $N=0.008\text{s}^{-1}$, filled circles: $N=0.011\text{s}^{-1}$, open squares: $N=0.014\text{s}^{-1}$, filled squares: $N=0.016\text{s}^{-1}$, crosses: $N=0.018\text{s}^{-1}$). The lines show power-law dependences of E on different Richardson numbers.

As may be inferred from the above relationships, the zero-order theory of Zilitinkevich [6] predicts for the equilibrium entrainment $Ri_b = C_e (1 + 2C_e)^{-1} Ri_N$ and $E = C_e Ri_b^{-1} = (1 + 2C_e) Ri_N^{-1}$. The LES results for this entrainment regime are shown in Fig. 2. The computations have been conducted with $B_s = 0.0098 \text{ m}^2 \cdot \text{s}^{-3}$ and N within the range of its atmospheric variability (from $N=0.0057 \text{ s}^{-1}$ to $N=0.018 \text{ s}^{-1}$). Concluding from the presented data, the LES yields $E = C_e Ri_b^{-1}$ with the value of the entrainment coefficient C_e about 0.17 that is very close to the laboratory and atmospheric estimate of C_e from [6]. The analogous relationships, $E \sim Ri_b^{-1}$, have been obtained in a series of recent LES studies of the CBL [1].

Note that Δb is generally smaller than the actual buoyancy increment δb across the inversion layer with the depth δz_i , and the ZOM entrainment flux B_i is not equal to the actual buoyancy flux of entrainment δB_i at level z_i , see Fig.1. Therefore, it looks reasonable to introduce the *Richardson number* $Ri_{\delta b} = (\delta b \cdot z_i) / w_*^2$ based on the actual buoyancy increment δb and evaluate dependence of E on this dimensionless parameter. Our LES experiments show (see Fig. 2) that such dependence has the form $E = C_{\delta e} Ri_{\delta b}^{-3/2}$, where the value of constant $C_{\delta e}$ is very

close to 1. Consequently, $Ri_{\delta b} \sim Ri_N^{2/3} \sim Ri_b^{2/3}$. These results cannot be explained in terms of ZOM that does not operate with δb and δz_i . In this connection, we suspect that in some cases reported in the literature, where dependence of E on Ri_b in the ZOM was found to be steeper than -1 law, this was due to inaccurate or incorrect evaluation of Δb from experimental data.

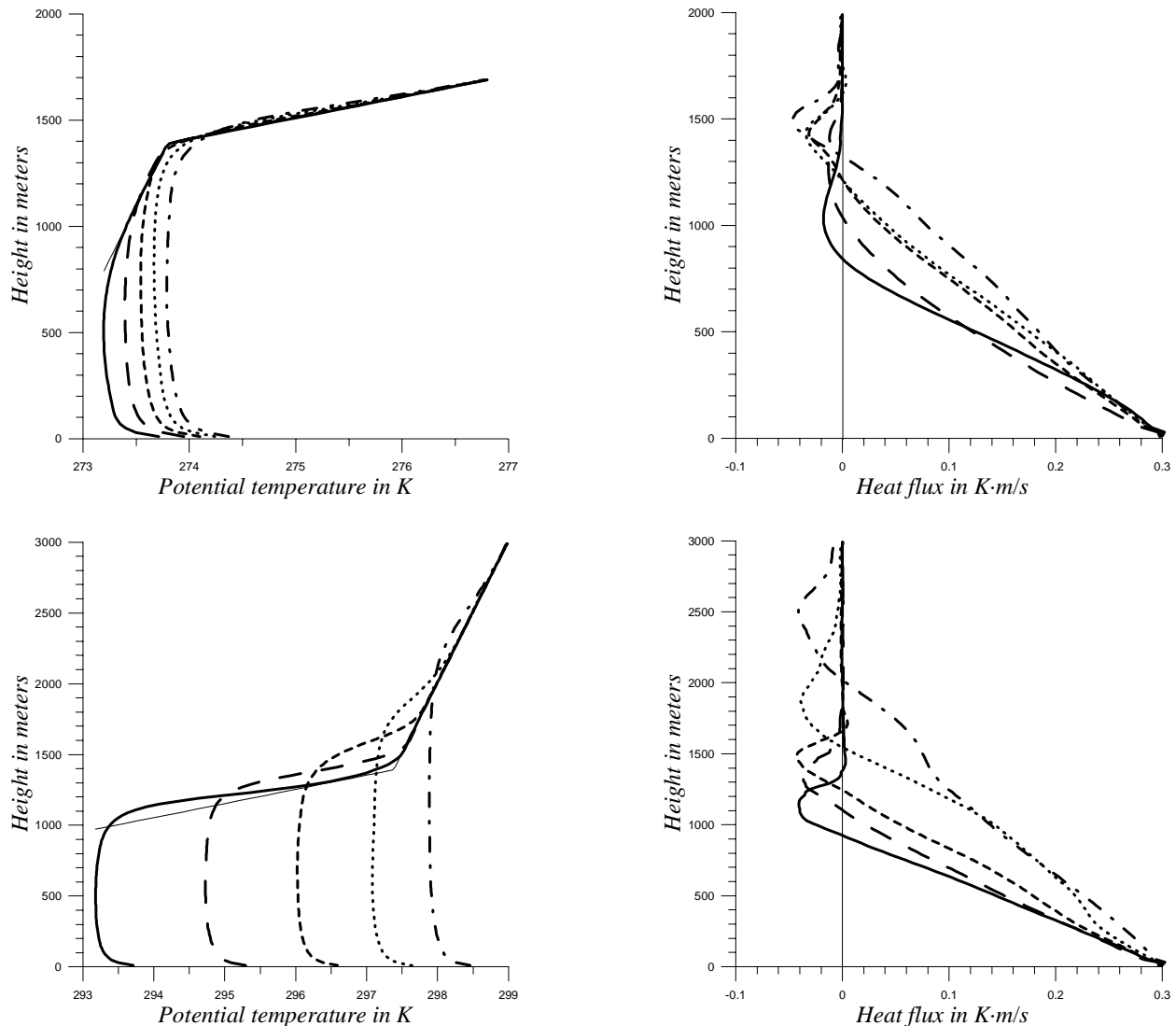


Figure 3. Evolution of temperature and heat flux profiles in the WS (upper plots, the time lag between profiles is about 500s) and SW (lower plots, the time lag is about 5000s) cases. The order of profiles in time: solid, long-dashed, short-dashed, dotted, dashed-and-dotted. Background profiles in the temperature plots are shown by thin lines.

ENTRAINMENT IN DISCRETELY STRATIFIED FLUID

We now consider the convective entrainment in the fluid system that consists of two adjacent layers. Each layer in this system has its own thermal stratification. A similar structure, in many

cases with more than two layers, is commonly observed in the lower portion of the earth's atmosphere above the CBL. We will be distinguishing between the weak-strong (WS) case, when the CBL first develops in the weakly stratified fluid (that is with small temperature/buoyancy lapse rate or small N) and then proceeds into the fluid with relatively strong stratification (that is with large temperature/buoyancy lapse rate or large N). The opposite configuration, when the strongly stratified fluid underlies the weakly stratified one, will be referred to as the strong-weak (SW) case.

Simulated temperature and heat flux profiles referring to different stages of the CBL evolution in discretely stratified fluid are demonstrated in Fig. 3. Note different time scales of the CBL growth in the WS and SW cases. The presented LES data show that the CBL growth (entrainment) rate and depth of the entrainment zone (this zone is signified by negative values of the heat flux) strongly vary in the vicinity of transition (bending) points of the background temperature profiles.

In the WS case, the CBL development stagnates as the temperature profile passes through the transition point. Such stagnation is manifested by almost coinciding heat flux profiles referring to two subsequent time moments separated by 500s. As can be inferred from the vertical displacement of the heat flux minimum, the CBL growth after the transition happens very slowly compared to the CBL development in the lower, weakly stratified fluid. In the strongly stratified environment, on the other hand, the maximum magnitude of the entrainment heat flux increases, but the entrainment zone shrinks.

It is seen in the presented plots and it can be also shown by direct evaluation of $z_i(t)$ and $\delta z_i(t)$ that in both WS and SW cases the evolution of the entrainment zone happens in a rather different manner to that in the case of equilibrium entrainment in the linearly stratified fluid. This requires development of new generation of entrainment parameterizations that will be able to adequately account for the nonstationarity of convective entrainment in heterogeneously stratified fluids.

REFERENCES

1. Stevens, B., and D. H. Lenschow, 2001: Observations, experiments, and large eddy simulation. *Bull. Amer. Meteor. Soc.*, **82**, 283-294.
2. Nelson, E., R. Stull, and E. Eloranta, 1989: A prognostic relationship for entrainment zone thickness. *J. Appl. Meteorol.*, **28**, 885-903.
3. Fedorovich, E. E., and D. V. Mironov, 1995: A model for shear-free convective boundary layer with parameterized capping inversion structure. *J. Atmos. Sci.*, **52**, 83-95.
4. Fedorovich, E., F. T. M. Nieuwstadt, and R. Kaiser, 2001: Numerical and laboratory study of horizontally evolving convective boundary layer. Part I: Transition regimes and development of the mixed layer. *J. Atmos. Sci.*, **58**, 70-86.
5. Lilly, D. K., 1968: Models of cloud-topped mixed layers under a strong inversion. *Quart. J. Roy. Meteorol. Soc.*, **94**, 292-309.
6. Zilitinkevich, S.S., 1991: *Turbulent Penetrative Convection*. Avebury Technical, Aldershot, 179 pp.
7. Deardorff, J. W., 1970: Convective velocity and temperature scales for the unstable planetary boundary layer and for Raleigh convection. *J. Atmos. Sci.*, **27**, 1211-1213.